MOLECULAR AND CELLULAR BIOLOGY, Aug. 2006, p. 5850–5860 Vol. 26, No. 15
0270-7306/06/$08.00+0 doi:10.1128/MCB.01854-05

A Distant Upstream Locus Control Region Is Critical for Expression of the Kit Receptor Gene in Mast Cells

Georgina Berrozpe,[1] Valter Agosti,[1] Christine Tucker,[1] Cedric Blanpain,[3] Katia Manova,[2] and Peter Besmer[1,4,5]*

Developmental Biology Program[1] and Molecular Cytology Facility,[2] Sloan-Kettering Institute, Howard Hughes Medical Institute, The Rockefeller University,[3] Gerstner Sloan-Kettering Graduate School of Biomedical Sciences,[4] and Weill Graduate School of Medical Sciences, Cornell University,[5] New York, New York 10021

Received 21 September 2005/Returned for modification 25 November 2005/Accepted 7 May 2006

The Kit receptor tyrosine kinase functions in hematopoiesis, melanogenesis, and gametogenesis and in interstitial cells of Cajal. We previously identified two upstream hypersensitive site (HS) clusters in mast cells and melanocytes. Here we investigated the roles of these 5′ HS sequences in *Kit* expression using transgenic mice carrying *Kit-GFP* reporter constructs. In these mice there is close correspondence between *Kit-GFP* reporter and endogenous *Kit* gene expression in most tissues analyzed. Deletion analysis defined the 5′ upstream HS cluster region as critical for *Kit* expression in mast cells. Furthermore, chromatin immunoprecipitation analysis in mast cells showed that H3 and H4 histone hyperacetylation and RNA polymerase II recruitment within the *Kit* promoter and in the 5′ HS region were associated with *Kit* expression. Therefore, the 5′ upstream hypersensitivity sites appear to be critical components of locus control region-mediated *Kit* gene activation in mast cells.

Differential control of gene expression during embryonic development and in the adult organism is mediated by the interaction of the transcription machinery with *cis* regulatory elements located at the promoter, upstream, or in intronic sequences of a gene. The mechanism by which tissue-specific gene expression is achieved involves the action of transcription factors together with changes in chromatin structure. Chromatin structure is a major determinant of gene expression, and mechanisms of chromatin remodeling are critical components of its regulation. Whereas SWI/SNF-like chromatin-remodeling ATPases disrupt histone-DNA interactions, covalent N-terminal histone modifications, including acetylation, methylation, and phosphorylation, also have important roles in the remodeling of chromatin structure and the regulation of transcription (36). In this way histone modification patterns have been proposed to constitute a histone "code" which specifies downstream functions (45). Hyperacetylation and hypoacetylation of histones H3 and H4 correlate with open/accessible or closed/inaccessible chromatin structures, respectively, and transcriptional activation or repression (22, 31). Thus, the characterization of histone modification patterns has become an important tool in studies of gene expression.

The Kit receptor tyrosine kinase (RTK) functions in distinct cell populations during embryonic development and in the postnatal animal (5, 6). During gametogenesis, *Kit* is expressed in primordial germ cells as they migrate from the allantois to the genital ridge (10, 35). Subsequently, during postnatal gametogenesis, *Kit* is expressed in spermatogonia and oocytes and in endocrine Leydig and thecal cells (2). In hematopoiesis during embryogenesis and in postnatal animals, Kit is expressed in hematopoietic stem cells and lineage progenitors, as well as in mast cells and eosinophils (5, 18, 48). In melanogenesis, *Kit* is expressed in migrating melanoblasts during embryonic development, in differentiated melanocytes in hair follicles, and in the gastrointestinal tract in interstitial cells of Cajal (7, 34, 41). *Kit* loss-of-function mutations affect hematopoiesis, melanogenesis, and gametogenesis, as well as the autonomous movement of the gastrointestinal tract. In summary, *Kit* expression is restricted to distinct cell types in which the Kit receptor functions. Studies of the mechanisms that control cell type-specific *Kit* expression are therefore of great significance.

The Kit RTK is encoded at the white spotting (*W*) locus on mouse chromosome 5 in the vicinity of the RTKs *PDGFR*α and *flk1* and comprises 21 exons contained in 70 kb (13, 19, 20, 39, 40). Many *W* mutations affecting *Kit* structure and function have been identified and characterized; the analysis of expression mutations has provided some insight into the mechanism of tissue-specific *Kit* expression. W^{sh} and W^{bd} mutant mice exhibit a pigmentation defect and lack tissue mast cells, but they are fertile and not anemic; furthermore, W^{bd} mice lack a functional network of interstitial cells of Cajal and intestinal pacemaker activity (15, 28, 29). In W^{sh} and W^{bd} mutant mice, *Kit* expression is diminished in hematopoietic progenitors in the bone marrow (BM) and lost in bone marrow-derived mast cells (BMMC). The W^{57} mutation is less severe, affecting melanogenesis and reducing mast cell numbers, and *Kit* expression is diminished in BM progenitors and BMMC, but like W^{sh}, this mutation does not affect erythropoiesis and gametogenesis (29). Our previous analysis of these mutations showed that the W^{sh} mutation arises from a 2-cM inversion on mouse chromosome 5 sequences 75 kb upstream of the *Kit* transcription start site, while W^{57} is a 110-kb deletion from approximately kb −147 to −34 from the *Kit* transcriptional start site (4, 15, 29). These observations suggested that the W^{sh} and W^{57} mutations affect 5′ upstream elements controlling *Kit* gene expression.

Locus control regions (LCRs) are *cis*-acting elements that

* Corresponding author. Mailing address: Memorial Sloan-Kettering Cancer Center, 1275 York Avenue, New York, NY 10021. Phone: (212) 639-8188. Fax: (212) 717-3623. E-mail: p-besmer@ski.mskcc.org.

determine normal levels of copy number-dependent and integration site-independent tissue-specific expression of a linked transgene in mice (21, 33). LCRs are composed of DNase I-hypersensitive sites containing binding sites for tissue-specific and ubiquitous transcription factors. The best-known example of an LCR is in the β-globin gene cluster, where the LCR regulates the expression of the different globin genes in a developmentally controlled order (11, 17). It would be of great interest to learn whether tissue-specific expression of the *Kit* gene is in part controlled by an LCR.

Previously, we identified two hypersensitive site clusters in bone marrow mast cells and melanocytes located at −147 to −154 kb and −21 to −28 kb upstream of the *Kit* transcription start site, respectively (4). DNase I-hypersensitive sites were also observed in the vicinity of the *Kit* transcription start site in the chromatin of *Kit*-expressing hematopoietic, melanocytic, and embryonic stem cells. In addition, a cluster of four hypersensitive sites has been detected in the middle of intron 1 in hematopoietic cells (12). In order to investigate the roles of the distant upstream sequences in *Kit* receptor expression in various cell systems, we have made transgenic mice carrying bacterial artificial chromosome (BAC) reporter constructs containing 200 kb upstream and 60-kb *Kit* coding sequences. In these mice, the reporter gene reflects the expression of the endogenous *Kit* gene in the brain, testis, oocytes, mast cells, and melanocytes, although no expression was observed in hematopoietic progenitors in bone marrow. We show that sequences within the 5′ upstream hypersensitive site cluster are critical for *Kit* expression in mast cells. We have also investigated molecular events associated with *Kit* activation in mast cells and determined the pattern of histone H3 and H4 acetylation and RNA polymerase II (Pol II) recruitment to the 5′ HS region and the *Kit* promoter. We propose that the 5′ upstream hypersensitivity sites are critical components of LCR-mediated *Kit* gene activation in mast cells.

MATERIALS AND METHODS

BACs, transgenes, and transgenic mice. All BACs used in this study were derived from the mouse BAC RP23-232H18 (BACPAC Resources), which includes 60 kb of *Kit* coding sequences and 200 kb of *Kit* 5′ upstream sequences. BAC RP23-232H18 was modified by using homologous recombination in bacteria (51) to include an enhanced green fluorescent protein (EGFP) (GFP) expression cassette at the *Kit* translation start site. A 500-bp EcoRI fragment and a 800-bp XbaI fragment corresponding to sequences 5′ and 3′, respectively, of the *Kit* translation start site and including the GFP reporter gene, was cloned into the SalI site of the pSV1-RecA shuttle vector and was used to transform bacteria containing the target BAC clone. Cointegrant and resolved clones were detected by Southern blot analysis. Clones with the expected restriction pattern were further analyzed by a panel of restriction enzymes, followed by Southern blotting and hybridization with probes corresponding to the homology arms and the GFP reporter gene. Furthermore, homologous recombination was used to generate targeted deletions within the initial *BAC200-Kit-GFP* construct (37). Regions of 500 bp on either side of the deletions were amplified from the modified *BAC200-Kit-GFP* clone. The PCR products were cloned in the pSV1-RecA shuttle vector to generate the targeting vectors. Clones containing the deletion were identified using PCR. Three constructs, *BAC30-Kit-GFP*, *BAC3-Kit-GFP*, and *BAC200-Δ5′HS-Kit-GFP* containing, respectively, 30 kb, 3 kb, and 200 kb, including the 5′ HS deletion (7-kb SacI fragment) and 60 kb of *Kit* coding sequence were generated. BAC DNA was prepared using the PSIΨCLONE BAC DNA isolation kit (Princeton Separations) following the manufacturer's instructions. After purification with Ultrafree-MC filter (Millipore 30-kilodalton molecular mass cutoff; catalog no. UFC3LTK25), circular DNA was diluted in injection buffer (0.1 M NaCl, 10 mM Tris, pH 7.5, 0.1 M EDTA) and microinjected into the pronuclei of C57BL/6 mouse zygotes. Microinjection was done at Sloan-Kettering Transgenic Core Facility. Transgenic founder animals were typed by using PCR with the following primers from the EGFP reporter gene: forward (5′-CAGAAGA ACGGCATCAAGGT-3′) and reverse (5′-GGCGGCGGTCACGAACTCCA 3′-). Transgenic founders were bred to C57BL/6 mice, and offspring were typed by PCR using GFP primers.

DNA analysis. Transgenic mouse lines were characterized by Southern blotting of tail DNA. Southern blotting and hybridization were carried out by standard procedures. Blots were scanned with a phosphorimager, and the results were used to calculate the transgene copy number. The integrity of transgenes was verified by pulsed-field gel electrophoresis. The preparation of samples for pulsed-field gel electrophoresis, enzyme digestions, and electrophoresis were performed as described previously (4, 15).

Cell culture. Mast cells from bone marrow of adult mice and 32D myeloid cells were grown in RPMI 1640 supplemented with 10% fetal calf serum, 10% conditioned medium from X63 interleukin 3 (IL-3)-producing cells, nonessential amino acids, and sodium pyruvate.

RNase protection assays. Total cellular RNA was extracted from tissues by RNAwiz (Ambion). T7 or T3 polymerase was used to prepare antisense mRNA transcripts from linearized plasmids (MAXIscript in vitro transcription kit; Ambion). GFP and *Kit* probes were fragments of 255 bp (GFP) and 370 bp (*Kit* exons 3 to 5), respectively. The transcripts were gel purified (5% acrylamide, 8 M urea denaturing gels) to isolate sense probes. The RNase protection experiments were performed using the RPA III RNase protection assay kit (Ambion). Protected RNA fragments were visualized with a phosphorimager.

Immunohistochemistry and microscopy. Paraffin sections (8 μm) from 4% paraformaldehyde-fixed tissues were processed for immunohistochemistry at the Molecular Cytology Core Facility of the Memorial Sloan-Kettering Cancer Center using Discovery staining module (Ventana Medical Systems). The incubation with the anti-GFP antibody (rabbit polyclonal antibody; Molecular Probes catalog no. A11122) was followed by biotinylated goat anti-rabbit immunoglobulin G (Vectasin ABC kit, catalog no. PK-6101). Diaminobenzidine was detected with a kit containing blocker D, copper D, inhibitor D, streptavidin-horseradish peroxidase D, and diaminobenzidine D (Ventana Medical Systems) and used according to the manufacturer's instructions. Imaging was carried with a Zeiss Axioplan 2 microscope, equipped with Qimaging Retiga EX charge-coupled device camera and Improvision image acquisition software. The dorsal trunk region from E11.5 (embryonic day 11.5) embryos was optically sectioned with a Leica TCS SP2 confocal microscope, using a 488-nm laser line.

Flow cytometry analysis. Monoclonal antibodies were from BD Pharmingen. Appropriately labeled isotype controls and single/double-color-stained cells were always used to define the specific gates. A FACScalibur or FACScan (BD Biosciences) was used for analysis.

BMMC, peritoneal mast cell, and melanocyte analyses. Bone marrow-derived mast cells were derived from total BM cells as previously described (1). Peritoneal mast cells were obtained by postmortem peritoneal lavage with 5 ml of phosphate-buffered saline (PBS). A total of 3×10^5 cells resuspended in 200 μl staining buffer (PBS without Ca^{2+} and Mg^{2+}, 3% fetal calf serum, 0.02% NaN_3) were incubated for 20 min at 4°C with 0.5 μg of murine Fc block (anti-mouse CD16/CD32 monoclonal antibody), followed by a 30-min incubation with 1 μg of allophycocyanin (APC)-conjugated anti-Kit monoclonal antibody. The cells were then washed, resuspended in 400 μl of staining buffer, and analyzed.

(i) Analysis of bone marrow cells. Bone marrow was flushed from femora with PBS, and a single-cell suspension was obtained by gentle pipetting and passage through a nylon strainer (Falcon). A total of 2.5×10^6 cells were resuspended in staining buffer and incubated for 15 min at 4°C with 1 μg of murine Fc block and then labeled with a mix of lineage-specific monoclonal antibodies (anti-mouse Ter119, B220, Mac-1, Gr-1, CD4, CD8, and CD3) conjugated to phycoerythrin (PE) and anti-Kit monoclonal antibody conjugated to APC. If necessary after incubation, mature red cells were depleted by hypotonic lysis (PharM Lyse; BD Pharmingen).

(ii) Sorting of lin^- Kit^+ cells. A total of 1×10^8 bone marrow cells from femora and tibias were stained with lineage-specific PE-conjugated monoclonal antibodies and APC-conjugated anti-Kit monoclonal antibody. Gated lineage-negative, Kit-positive (lin^- Kit^+) bone marrow cells were sorted by a FACSVantage flow cytometer (BD Biosciences) or MoFlow sorter (Cytomation). Purification of the skin cells was performed as described previously (8). Briefly, skin from 4- to 5-day-old mice was incubated with collagenase (Sigma) following trypsinization. Neutralized cell suspension was obtained by passing the cells throughout 70-μm and 40-μm strainers (Falcon). A total of 5×10^6 cells resuspended in staining buffer were labeled with a specific monoclonal antibody, biotin-conjugated rat anti-mouse CD117 (c-kit) and APC-conjugated anti-CD45 monoclonal antibody (BD Pharmingen). Cells were gated for single events and viability and then sorted according to their expression of $CD45^+$/Kit^+/GFP and

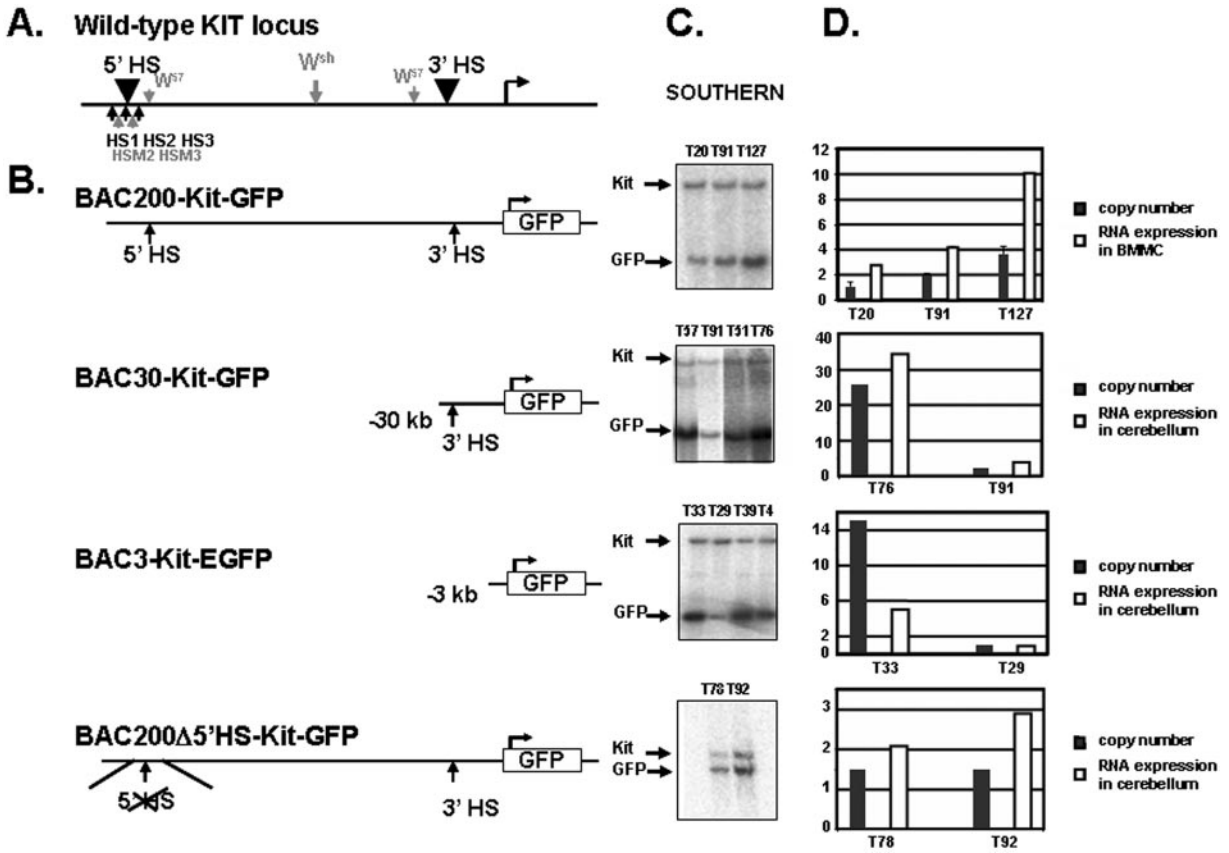

FIG. 1. Derivation of transgenic mice carrying *BAC-Kit-GFP* reporter constructs. (A) Schematic representation of the mouse *Kit* locus. Black arrowheads above the locus indicate the positions of the mast cell HS clusters. Arrows below the locus show the localization of the mast cell-specific HSs (black) and melanocyte-specific HSs (gray). (B) A GFP reporter was placed at the *Kit* translation start site in exon 1 of the BAC RP23-232H18 (*BAC200-Kit-GFP*). The *BAC200-Kit-GFP* construct includes 200 kb 5′ upstream sequences and 60-kb *Kit* coding sequences. Arrows indicate the positions of the 5′ and 3′ HS clusters. The *BAC30-Kit-GFP* and *BAC3-Kit-GFP* constructs include 30 and 3 kb of 5′ upstream sequences of the *Kit* gene, respectively. In *BAC200-Δ5′HS-Kit-GFP*, the 5′ HS cluster sequences (7 kb) were deleted. (C) Determination of transgene copy numbers by Southern blot analysis in transgenic mice carrying the four different constructs. DNA from cerebellum was digested with SpeI and hybridized with a probe located at the 5′ end of the BAC-RP23-232H18. The transgenic lines carrying the different constructs are indicated. (D) Copy number-dependent expression of the GFP transgene. The ratios of the DNA signals of the GFP transgene versus endogenous Kit gene were determined with a phosphorimager and are represented in the histogram by black bars. Error bars represent the standard deviations from three independent Southern analyses. The ratios of GFP RNA versus endogenous *Kit* RNA expression levels in BMMC (*BAC200-Kit-GFP* mice) and in cerebellum (*BAC30-Kit-GFP*, *BAC3-Kit-GFP*, and *BAC200-Δ5′HS-Kit-GFP*) were determined with a phosphorimager. GFP expression levels are shown as white bars.

$CD45^-/Kit^+$/GFP. Fluorescence-activated cell sorting (FACS) analyses were performed either on FACSort or BD LSR (BD Biosciences).

ChIP and DNA analyses. Chromatin immunoprecipitation (ChIP) experiments were performed according to a protocol provided by Upstate Biotechnology. For ChIP with BMMC and 32D cells, 10^6 cells were used per immunoprecipitation. Briefly, the cells were cross-linked with 1% formaldehyde, collected, and washed with PBS containing protease inhibitors. The cells were resuspended in 200 μl sodium dodecyl sulfate lysis buffer on ice for 10 min and then sonicated with 8 sets of 12-second pulses by a Branson Sonifier 250 cell sonicator to an average DNA size of 600 to 1,000 bp. Antibodies against acetyl-histone H4 and acetyl-histone H3 were purchased from Upstate Biotechnology, and rabbit anti-RNA polymerase II was obtained from Santa Cruz Biotechnology. DNAs were phenol-chloroform extracted and ethanol precipitated. Five percent (by volume) of the immunoprecipitated material was used as a template for semiquantitative radiolabeled PCR; 25 cycles of amplification were followed by the addition of 0.125 mCi [α-^{32}P]dCTP. PCR products were resolved on 4.5% acrylamide gels, dried, and exposed on a phosphor screen, and images were quantitated by ImageQuant.

Primers. Oligonucleotides for the constructs were as follows: for *BAC200-Kit-GFP*, HomologyA (5′-GGAATTCTTACTGAGGTCAGGGGTG-3′ and 5′-GGAATTCCATCGCGGTGGCTGCGCTAG-3′) and HomologyB (5′-GCTCTAGAGCGCCTGGGATCTGCTCTGC-3′ and 5′-GCTCTAGAGCTGCAGAGAGGGGCGAGCC-3′); for *BAC30-Kit-EGFP*, HomologyA (5′-GACATCAGAGTCGACGGCATTTTTGATACATAA-3′ and 5′-TCTCATTTAGTTGACACTCTTCTCTTTTTG-3′) and HomologyB (5′-GAGAAGAGTGTCAACTAAATGAGACCTTGCTT-3′ and 5′-GACATCAGAGTCGACATGCCCTGTGAGAACTTGAC-3′); for *BAC3-Kit-GFP*, HomologyA (5′-GACATCAGAGTCGACGGCATTTTTGATACATAA-3′ and 5′-TGTGAATAGGTTGACACTCTTCTCTTTTTG-3′) and HomologyB (5′-GAGAAGAGTGTCAACCTATTCACATCCAACAC-3′ and 5′-GACATCAGAGTCGACACCCACCTCACATCTCCTTA-3′); and for *BAC200Δ5″HS-Kit-GFP*, HomologyA (5′-GACATCAGAGTCGACCACCTATCCTGACCATCC-3′ and 5′-TTGCCTGCTATTCCAACAACTAAAACACAT-3′) and HomologyB (5′-TTTAGTTGTTGGAATAGCAGGCAAAACAGG-3′ and 5′-GACATCAGAGTCGACTCATCAAGGTGGAAGCAT-3′).

Primers to identify the deletion constructs were as follows: for *BAC30-Kit-GFP*, 5′-GGCATTTTTGATACATAA-3′ and 5′-GTGGGGGAGAAACTACAAAC-3′; for *BAC3-Kit-GFP*, 5′-GGCATTTTTGATACATAA-3′ and 5′-CACCCCCTAAGCACATTCCT; and for *BAC200Δ5″HS-Kit-GFP*, 5′-TAATCCAAGGTTCATGCCC-3′ and 5′-AGGTTCAGAGGTTCGGTCCA-3′.

Oligonucleotides for ChIP were as follows: P1, 5′-TCCCCAGACTTTACAATA-3′ and 5′-TGCCAACCTCATCATACT-3′; P2, 5′-AAACAGCACAAGCCAAGC-3′ and 5′-GGGATTCGGAGATTACAG-3′; P3, 5′-GTCAGCAGGCGGTTCA

TABLE 1. Transgene copy numbers in *BAC200-Kit-GFP*, *BAC30-Kit-GFP*, *BAC3-Kit-GFP*, and *BAC200-Δ5′HS-Kit-GFP* transgenic mice[a]

BAC construct	Transgenic mouse line	No. of transgene copies
BAC200-Kit-GFP	T20	2
	T91	4
	T127	8
BAC30-Kit-GFP	T51	11
	T57	50
	T76	50
	T93	4
BAC3-Kit-GFP	T4	27
	T29	2
	T33	30
	T39	14
	T71	1
BAC200-Δ5′HS-Kit-GFP	T78	3
	T92	3

[a] Transgene copy numbers were determined by comparing *Kit-GFP* and endogenous *Kit* signals from Southern blot analyses of genomic DNA using a phosphorimager (Bio-Rad).

TC-3′ and 5′-GAGGTGGGGAGTGGAGTG-3′; P4, 5′-TGTCATTCACTCTTC CTG-3′ and 5′-TTGCTTGTTTACTGTTTG-3′; P5, 5′-CACAAAGGACAAAAA CAT-3′ and 5′-ATCAGGTATCAGCAAGGT-3′; P6, 5′-TTTCTTCAGTGGTGT AGC-3′ and 5′-TCTCCCGTTTCCTCGTTA-3′; P7, 5′-GAGTGAGCATCCCTA CCA-3′ and 5′-TGTGAACCTTATCCTTAT-3′; P8, 5′-CTGGCGATTCATTTG GTA-3′ and 5′-CTGGGGTCTTTCACACAT-3′; P9, 5′-CCAAAGAAACTAAAC TGC-3′ and 5′-ATCATCCAACGAAGAATC-3′; Promoter 1, 5′-AACACCTCCA CCATAAGC-3′ and 5′-TAGCACTCTCCCTCCATC-3′; Promoter 2, 5′-AGGCA GCGGGAGGGAGTG-3′ and 5′-TTGTGGCCGTTTACGTCG-3′; P3 EGFP, 5′-CAGAAGAACGGCATCAAGGT-3′ and 5′-GGCGGCGGTCACGAACTCCA-3′; Promoter 4, 5′-AGGCAGCGGGAGGGAGTG-3′ and 5′-GAGCAGGACCAACAG GAC-3′; and Promoter 5, 5′-AGGCAGCGGGAGGGAGTG-3′ and 5′ CCATCGC GGTGGCTGCGCTAG-3′.

RESULTS

Generation of BAC transgenic mice carrying *Kit-GFP* reporter constructs. In order to identify *cis*-acting control elements involved in the transcriptional regulation of the *Kit* gene, we carried out a functional analysis using BAC transgenic mice. We identified a clone from a mouse BAC library (RP23-232H18) containing 60 kb of coding sequences and 200 kb of 5′ upstream sequences of the *Kit* gene (27). Subsequently, by using bacterial homologous recombination methodology (50), the BAC clone was modified by inserting an EGFP reporter gene (GFP) at the *Kit* translation start site in exon 1, as shown in Fig. 1. The resulting recombinant BAC was characterized extensively by restriction mapping using standard and pulsed-field gel electrophoresis. These analyses confirmed the presence of the targeted modification and failed to reveal any rearrangements or deletions in the modified *BAC200-Kit-GFP* clone. DNA from the *BAC200-Kit-GFP* clone was analyzed for integrity by pulsed-field gel electrophoresis and then microinjected into fertilized mouse oocytes to produce transgenic founder animals. Tail DNA prepared from founder offspring (F_o) was screened by PCR for the presence of the GFP gene, and transgene copy numbers were determined by Southern blot analysis (Fig. 1; Table 1). To confirm the integrity of the transgene in the three transgenic lines carrying the *BAC200-Kit-GFP* construct (lines T20, T91, and T127), high-molecular-weight DNA recovered from the spleen of F_1 animals was embedded in agarose plugs and then analyzed by pulsed-field gel electrophoresis and blot hybridization. The GFP gene and a 500-bp fragment corresponding to the 5′ end of the BAC clone were used as probes to detect the NotI restriction fragment predicted from integration of the intact *BAC200-Kit-GFP* clone. The two probes detected the 200-kb NotI band in all three lines, indicating that each transgenic mouse line carried nonfragmented copies of the transgene.

Expression analysis of *BAC200-Kit-GFP* transgenic mice. To determine whether the *BAC200-Kit-GFP* transgene mirrored endogenous *Kit* mRNA expression, we analyzed GFP reporter gene expression in different tissues using RNase protection assays. *Kit-GFP* reporter expression was evident in the cerebellum, testis, bone marrow-derived mast cells, and ovary, but not in the liver in the three lines analyzed. Analysis of these tissues from one line, T20, carrying two copies of the transgene is shown in Fig. 2A. Close correspondence between the expression of *Kit-GFP* reporter genes and endogenous *Kit* genes was observed in these tissues, except in the ovary where the level of transgene expression was lower than expected. Furthermore, *Kit-GFP* transgene expression was analyzed in BMMC of the three *BAC200-Kit-GFP* lines relative to the levels of endogenous *Kit* expression. By RNase protection assay and by FACS analysis, all three lines were positive for *Kit-GFP* expression. In addition, FACS analysis showed that 80% or more of the Kit-positive BMMC were also GFP positive (Fig. 4). Thus, the transgene was expressed in all lines irrespective of its site of integration, and the levels of expression were closely related to transgene copy number (Fig. 1 and 2A).

To further evaluate *Kit-GFP* reporter gene expression in tissues of transgenic mice, we performed immunohistochemical analysis on sections of adult organs using an anti-GFP antibody (Fig. 2B). Consistent with the known pattern of the endogenous *Kit* expression, *Kit-GFP* transgene expression was detected in the cerebellar stellate and basket neurons and their axons. In the adult testis, transgene expression was confined to spermatogonial cells and Leydig cells. In the ovary, *Kit-GFP* expression was observed in oocytes at all stages of follicle development but was absent in thecal cells (Fig. 2B). In E11.5 embryos, *BAC200-Kit-GFP* transgene expression was observed in primordial germ cells in the mesentery and gonadal ridges (Fig. 2B) and in melanoblasts (not shown) by using confocal microscopy, again in agreement with endogenous *Kit* expression. Expression was highly tissue specific and did not extend to surrounding tissues. In addition, *Kit-GFP* reporter expression was examined in mast cells and melanocytes from dorsal skin of the T20 transgenic mouse line. Single-cell suspensions from back skin of 4-day-old transgenic mice were prepared and analyzed by FACS (Fig. 3). Two positive populations were detected: GFP^{high} cells expressing CD45 and Kit, presumptive mast cells, and GFP^{low}, Kit^+, $CD45^-$ cells corresponding to melanocytes.

GFP reporter gene expression was also analyzed in hematopoietic progenitors in the bone marrow by FACS in the three *BAC200-Kit-GFP* transgenic lines. Kit-positive cells were present in the lin^- subset of cells in the adult BM (5, 9, 30). As expected, no GFP-positive cells were detected in the Kit-neg-

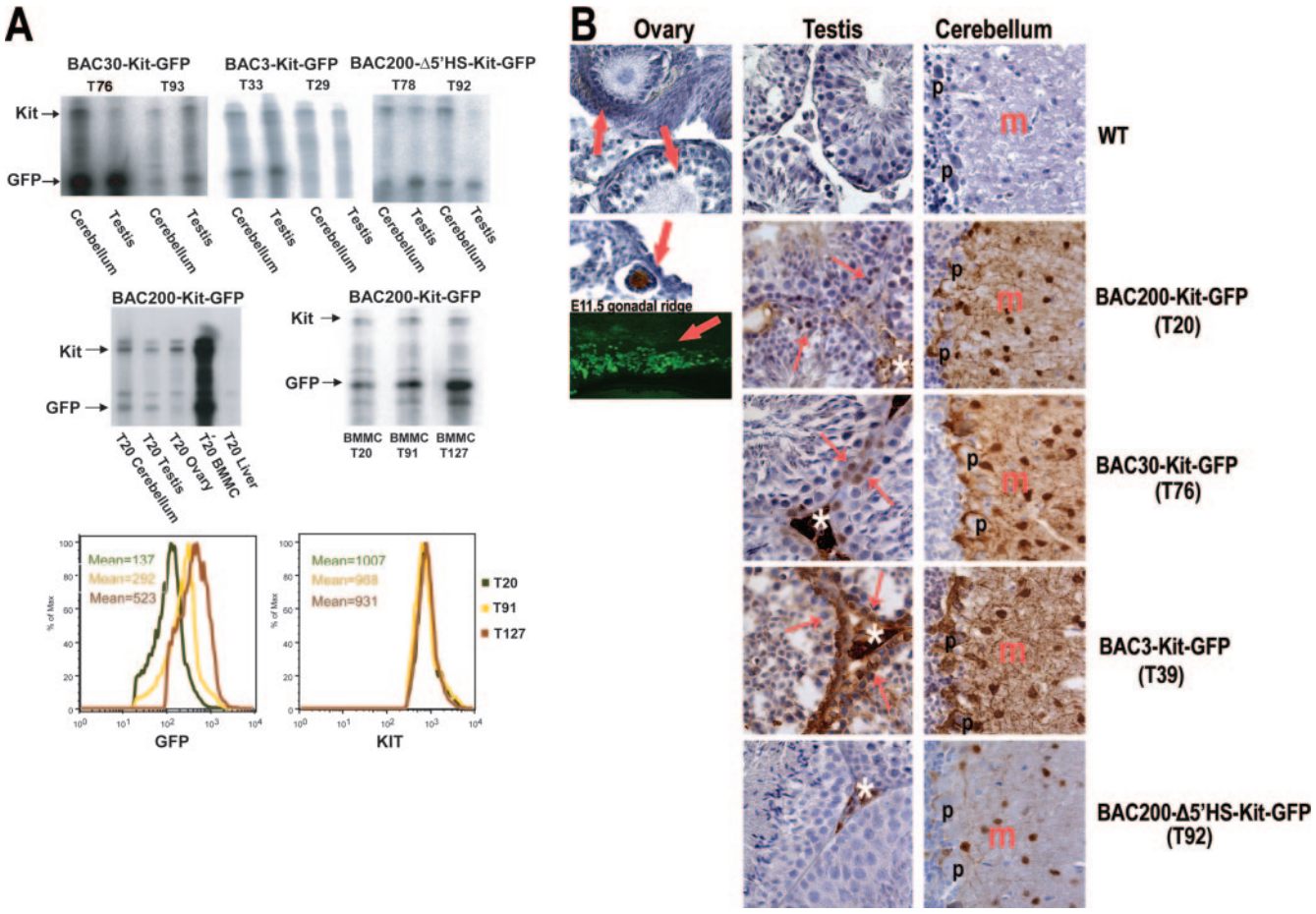

FIG. 2. GFP reporter expression in *BAC-Kit-GFP* transgenic mice. (A) RNase protection assay. Total RNA from cerebellum, testis, ovary, and liver (as indicated) of *BAC200-Kit-GFP*, *BAC30-Kit-GFP*, *BAC3-Kit-GFP*, and *BAC200-Δ5′HS-Kit-GFP* transgenic mice was processed for RNase protection assay using ^{32}P-labeled riboprobes specific for GFP and endogenous *Kit* RNA. Analysis of *Kit-GFP* and endogenous Kit expression in BMMC from T20, T91, and T127 *BAC200-Kit-GFP* mice by RNase protection and FACS analysis is shown. Mean values of fluorescence are indicated. Max, maximum. (B) Immunohistochemical detection of *Kit-GFP* transgene expression with anti-GFP antibody (signal in brown; hematoxylin counterstain in blue). Oocytes in the control ovary have no signal, while in the *BAC200-Kit-GFP* transgenic ovary, oocytes are stained in brown (red arrows). Representative sections of testis and cerebellum from nontransgenic and *BAC200-Kit-GFP*, *BAC30-Kit-GFP*, *BAC3-Kit-GFP*, and *BAC200-Δ5′HS-Kit-GFP* transgenic mice are shown. In the testis, *Kit-GFP* expression is found in spermatogonia (red arrow), and white stars show GFP expression in Leydig cells. The molecular layer (m) of the cerebellum shows staining in basket and stellate cell bodies as well as axons and dendrites. In addition, the molecular layer neurons form brown baskets around Purkinje cell bodies (p). Confocal microscopy identifies primordial germ cells in the mesentery and the gonadal ridge of E11.5 *BAC200-Kit-GFP* mouse embryos (red arrow).

ative fraction; however, only a small fraction (13%) of the lin$^-$ Kit$^+$ population expressed the GFP reporter (Fig. 4A). To further investigate the characteristics of the Kit$^+$ GFP$^+$ and Kit$^+$ GFP$^-$ cells, both populations were sorted by FACS. The two fractions were then grown in medium supplemented with IL-3 to produce BMMC. After 4 weeks in culture, only the Kit$^+$ GFP$^-$ cells gave rise to BMMC. Significantly, the BMMC derived from the GFP-negative subpopulation expressed high levels of the GFP transgene, demonstrating that the *Kit-GFP* reporter is turned on upon differentiation into mast cells (Fig. 4B). Taken together, these results suggest that the *BAC200-Kit-GFP* transgene includes most of the regulatory sequences required for cell type-specific *Kit* expression in primordial germ cells and melanoblasts during embryonic development, in oogenesis, and in the testis, in the cerebellum's basket and stellate neurons, in mast cells, and in melanocytes, but not in hematopoietic progenitors in the bone marrow and the fetal liver (not shown) and in thecal cells of the ovary.

Distant upstream sequences are required for *Kit* expression in mast cells. To further define the roles of upstream regulatory sequences in cell type-specific *Kit* expression, we used bacterial homologous recombination to generate three *Kit-GFP* reporter constructs with 30 kb (*BAC30-Kit-GFP*) and 3 kb (*BAC3-Kit-GFP*) of 5′ upstream sequences, respectively (37). In addition, a construct, *BAC200Δ5′HS-Kit-GFP*, was made in which the 5′ HS cluster region, a 7-kb (kb −147 to −154) SacI fragment, was deleted (Fig. 1B). Transgenic mice carrying these constructs were obtained, the integrity of the transgenes was characterized, and the copy number was determined as described above (Table 1). We obtained the following transgenic mouse lines: four lines with *BAC30-Kit-GFP* (T51, T57, T76, and T93), five lines with *BAC3-Kit-GFP* (T4, T29, T33,

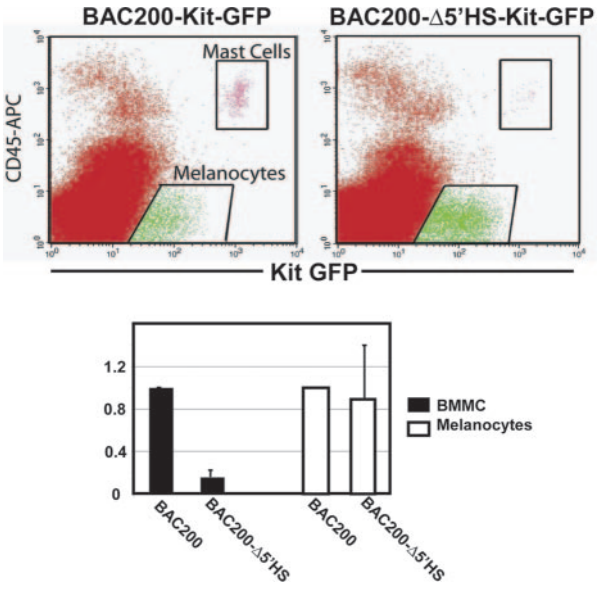

FIG. 3. Kit-GFP reporter expression in mast cells and melanocytes in P4 back skin of *BAC200-Kit-GFP* (T20) and *BAC200-Δ5′HS-Kit-GFP* transgenic mice (T92). Cell suspensions of dorsal skin were stained with APC-conjugated anti-Kit and anti-CD45 antibodies, and cells were analyzed by FACS on the basis of Kit, CD45, and GFP expression. In the bar graph, the numbers of Kit^+ $CD45^+$ (mast cell subset) and Kit^+ $CD45^-$ (melanocyte subset) cells expressing Kit-GFP from *BAC200-Δ5′HS-Kit-GFP* mice relative to the numbers of Kit-GFP expressing Kit^+ $CD45^+$ and Kit^+ $CD45^-$ cells from *BAC200-Kit-GFP* mice are shown. The standard deviations are indicated by the error bars ($n = 3$).

T39, and T71), and two lines with *BAC200Δ5′HS-Kit-GFP* (T78 and T92).

Analysis of GFP reporter gene expression in these mice was again determined by RNase protection, FACS, and immunohistochemistry. In the *BAC30-Kit-GFP* mice, *Kit-GFP* reporter expression in cerebellum, testis, and ovary was comparable to that in mice carrying the intact *BAC200-Kit-GFP* transgene and expression remained copy number dependent (Fig. 1 and Fig. 2A and B). Therefore, the regulatory sequences controlling *Kit* expression in these tissues are located within the *BAC30-Kit-GFP* construct. However, none of the transgenic lines (T51, T57, T76, and T93) expressed the *Kit-GFP* reporter in BMMC and in hematopoietic progenitors in the bone marrow (Fig. 4A). These observations indicate that additional 5′ upstream sequences not present in the *BAC30-Kit-GFP* transgene are necessary for *Kit* expression in mast cells. Analysis of *Kit-GFP* reporter expression in the cerebellum and testis of *BAC3-Kit-GFP* transgenic mice showed that expression levels were lower than expected in mice with multicopy transgenes (Fig. 1 and Fig. 2A and B). Evidence for ectopic *Kit* expression was observed in the ovary of one of the lines. None of these transgenic lines (T4, T29, T33, T39, and T71) expressed the transgene in mast cells (Fig. 4A). Importantly, neither one of the two *BAC3-Kit-GFP* mice carrying only one or two copies of the transgene expressed the *Kit-GFP* reporter in any tissue analyzed (Fig. 2A). Thus, proximal regulatory elements appear to be insufficient to drive *Kit-GFP* reporter expression in a reproducible fashion and at wild-type (WT) levels.

We had previously identified a hypersensitive site cluster located between kb −147 and −154 (HS1, -2, and -3 and HSm2 and -m3) upstream of the *Kit* transcription start site in mast cells and melanocytes. FACS analysis of BMMC, peritoneal, and skin mast cells and melanocytes from *BAC200-Δ5′HS-Kit-GFP* mice, which lack these sequences, showed no GFP expression in BMMC and severely reduced reporter gene expression in skin (Fig. 3 and 4A) and peritoneal mast cells (not shown). However, the number of melanocytes expressing the GFP reporter in 4-day-old T92 *BAC200-Δ5′HS-Kit-GFP* mice was comparable to that in T20 *BAC200-Kit-GFP* mice (Fig. 3). Taken together, these results provide evidence that the 5′ HS cluster sequences are essential for *Kit* expression in mast cells but not in melanocytes. Analysis of *Kit-GFP* reporter expression in the cerebellum of *BAC200-Δ5′HS-Kit-GFP* mice was analogous to that in mice carrying the intact *BAC200-Kit-GFP* transgene, although specific staining in the molecular layer appeared to be somewhat reduced compared to that in the *BAC200-Kit-GFP* mice. However, in the testis only, Leydig cells were stained, while spermatogonia lacked signal in the two different lines analyzed (Fig. 2B).

Histone H3 and H4 hyperacetylation in the 5′ HS cluster region correlates with an open chromatin structure. Enhancers and promoters of transcriptionally active genes are associated with open chromosomal regions, which are sensitive to nuclease digestion of DNase I-hypersensitive sites (49). In addition, modification of histones H3 and H4 is associated with gene activation in a number of systems and tends to be maximal at known regulatory sequences. To further define the chromatin structure in the 5′ HS cluster of the *Kit* gene, we characterized histone acetylation using chromatin immunoprecipitation. Formaldehyde-cross-linked chromatin from BMMC was immunoprecipitated with antibodies specific for the acetylated forms of histones H3 and H4. The amount of immunoprecipitated DNA was quantitated by semiquantitative PCR, using primers spanning the regions of interest, comparing the PCR products of the immunoprecipitated DNA and input DNA. The overall levels of H3 and H4 acetylation were assessed in the 5′ HS cluster of BMMC from WT and $W^{sh/sh}$ mice, in Kit-negative myeloid 32D cells and in Kit-expressing lin^- Kit^+ BM progenitor cells. In mast cells from WT and $W^{sh/sh}$ mice, H3 and H4 acetylation levels were shown to be two- and eightfold higher than in 32D cells, indicating a correlation between H3 and H4 hyperacetylation and an open chromatin structure in the 5′ HS cluster (Fig. 5). The mast cell specificity of the acetylation pattern was established by comparing these results with those obtained from analysis of lin^- Kit^+ hematopoietic progenitors isolated from BM. ChIP assays of lin^- Kit^+ hematopoietic progenitors revealed no acetylation enrichment in the 5′ HS cluster (Fig. 5).

To evaluate the relation between histone acetylation and transcriptional activation, we also characterized the histone acetylation status of the proximal *Kit* promoter. High levels of H3 and H4 acetylation were detected in Kit-expressing BMMC and in lin^- Kit^+ BM cells. In contrast, in Kit-negative mast cells from $W^{sh/sh}$ mice and in 32D cells, histone H3 and H4 acetylation levels were not increased (Fig. 6). Taken together, these data indicate that whereas acetylation in the 5′ HS cluster region correlates with *Kit* expression in mast cells, hyper-

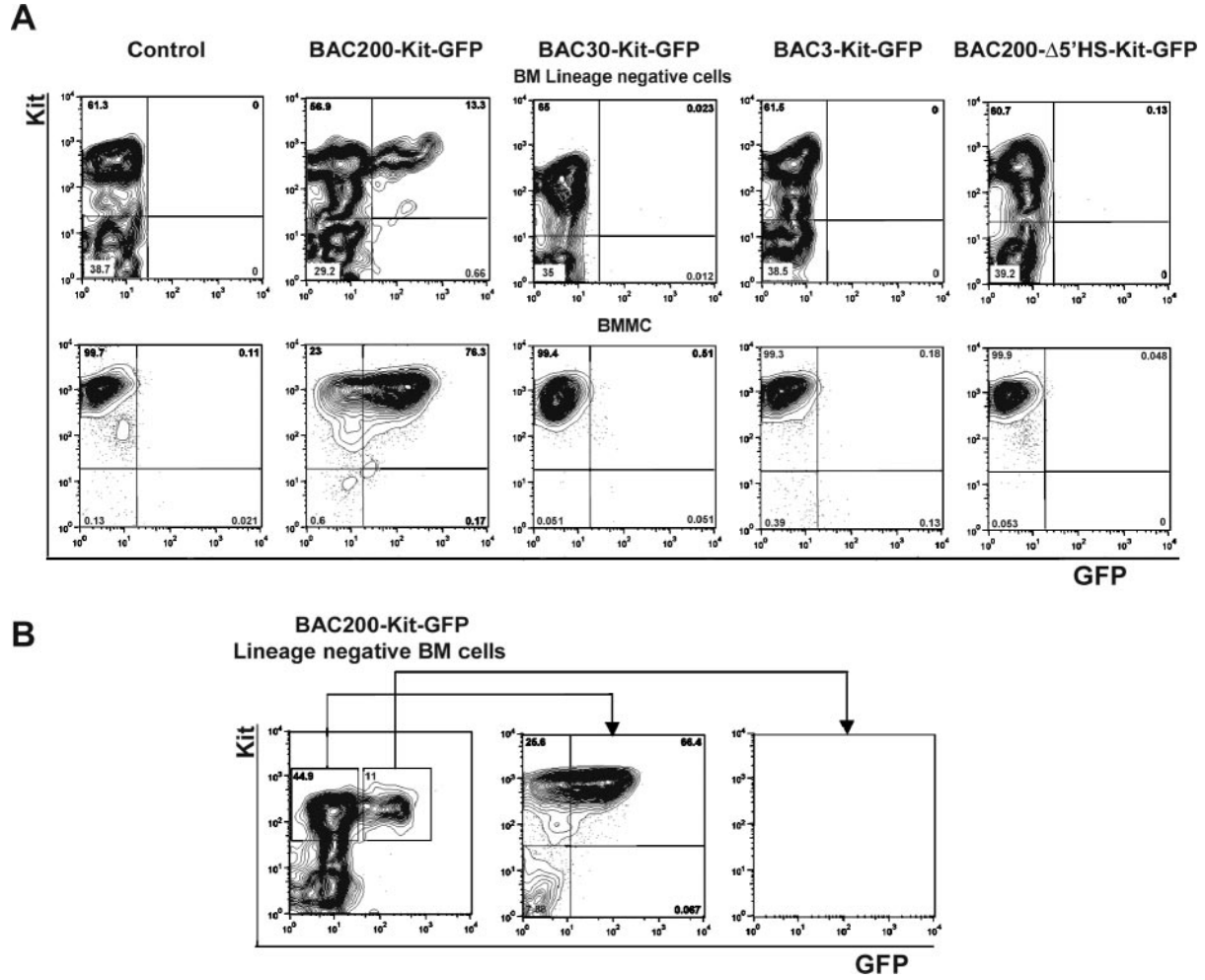

FIG. 4. Representative flow cytometric analysis of GFP expression in bone marrow progenitor cells (BM) and in bone marrow-derived mast cells of *BAC200-Kit-GFP* (T20), *BAC30-Kit-GFP* (T93), *BAC3-Kit-GFP* (T29), and *BAC200-Δ5′HS-Kit-GFP* transgenic mice (T92). (A) BM cells were stained with PE-conjugated anti-Lin and APC-conjugated anti-Kit antibodies, and cells within the lin^- gate were analyzed on the basis of Kit and GFP expression. Only a small fraction (13%) of the Kit^+ cells expressed the GFP in the *BAC200-Kit-GFP* transgenic mice. No GFP expression was found in lin^- Kit^+ BM cells of *BAC30-Kit-GFP*, *BAC3-Kit-GFP*, and *BAC200-Δ5′HS-Kit-GFP* transgenic mice in all the transgenic lines analyzed. BMMC were stained with APC-conjugated anti-Kit antibody and analyzed for Kit and GFP expression. Expression of the GFP reporter was detected only in the BMMC of the *BAC200-Kit-GFP* transgenic mice. (B) Kit^+ GFP^+ and Kit^+ GFP^- lin^- Kit^+ BM cells from *BAC200-Kit-GFP* transgenic mice were sorted by FACS. After 3 weeks of culture in IL-3-containing medium, only the Kit^+ GFP^- cells gave rise to BMMC expressing the GFP transgene. Kit^+ GFP^+ cells die after 3 days in culture.

acetylation in the promoter region correlates with *Kit* gene expression in mast cells and in hematopoietic progenitor cells.

Deletion of the 5′ HS region abolishes histone H3 and H4 hyperacetylation at the *Kit* promoter. We also investigated the consequences of deletion of the upstream regulatory sequences on chromatin structure in the *Kit* promoter and determined the pattern of acetylation of histones H3 and H4 in the *Kit* promoter of BMMC isolated from $W^{sh/sh}$ mice, which lack endogenous *Kit* expression, carrying either the *BAC200-Kit-GFP*, *BAC30-Kit-GFP*, or *BAC200-Δ5′HS-Kit-GFP* transgene. Strong hyperacetylation was observed in the *Kit* promoter sequences and in the GFP-coding sequences in BMMC of $W^{sh/sh}$ mice carrying the *BAC200-Kit-GFP* transgene. In contrast, no H3 and H4 hyperacetylation was apparent in BMMC isolated from $W^{sh/sh}$ carrying the *BAC30-Kit-GFP* or *BAC200-Δ5′HS-Kit-GFP* transgene (Fig. 6). The loss of H3 and H4 hyperacetylation in these BMMC was consistent with a lack of GFP expression in the mast cells of both transgenic lines. Therefore, these results imply that, in mast cells, both histone acetylation in the promoter region and transcriptional activation of the *Kit* gene require a functional 5′ HS cluster.

Recruitment of RNA Pol II to the 5′ HS cluster and promoter region in mast cells. RNA polymerase II has been reported to associate with distal upstream transcriptional control elements in several model systems (25, 42, 47). A long-range transfer mechanism in which Pol II is first recruited to the upstream regulatory element and then transferred to the promoter has been proposed. To further characterize the 5′ HS cluster and its role in the transcriptional regulation of the *Kit* gene, we sought to determine whether Pol II is recruited to this region. Using ChIP analysis and semiquantitative PCR with primers spanning this region, we measured Pol II binding in

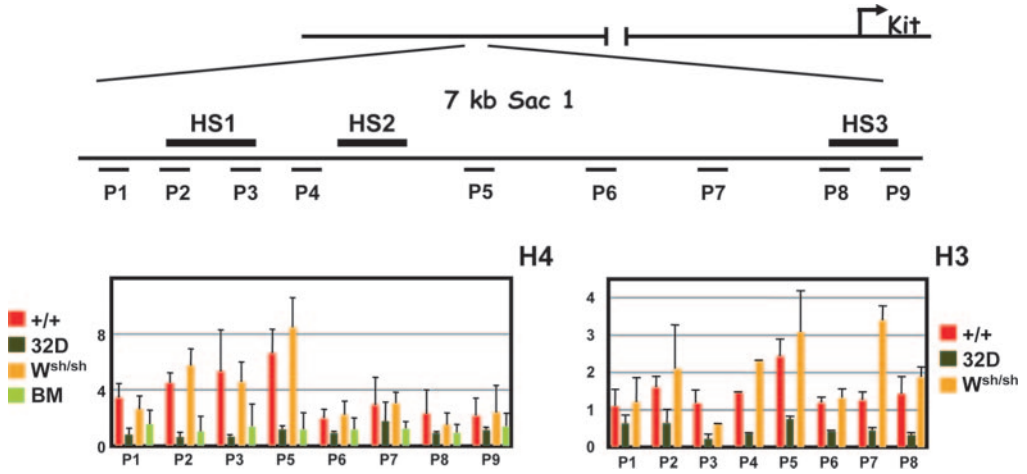

FIG. 5. Analysis of histone H3 and H4 acetylation in the chromatin of the 5′ HS cluster region. Formaldehyde-cross-linked chromatin obtained from WT (+/+) BMMC, W^{sh}/W^{sh} BMMC, 32D cells, and lin$^-$ Kit$^+$ BM cells was immunoprecipitated with antibodies directed against acetylated forms of histones H3 and H4, and the amount of the immunoprecipitated and input DNA was assayed by semiquantitative PCR. A schematic representation of the *Kit* locus is shown at the top. The positions of the different PCR amplification units (P1 to P9) on the 7-kb SacI fragment are indicated by horizontal bars. The ratios of signals of bound versus input chromatin were determined with a phosphorimager and are represented in the histogram. The error bars represent the standard deviations from three independent ChIP experiments.

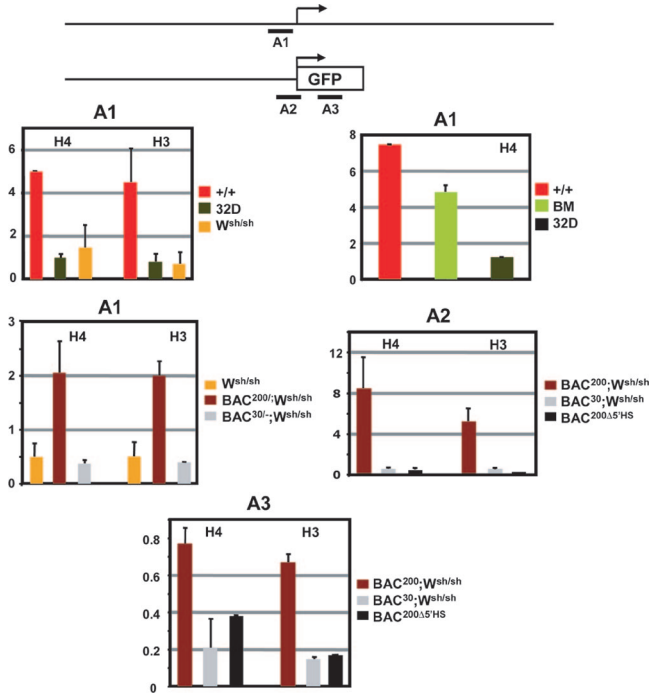

FIG. 6. Analysis of histone H3 and H4 acetylation in the chromatin of the proximal *Kit* promoter and the GFP reporter gene. A schematic representation of the endogenous *Kit* promoter and the transgene constructs is shown at the top. The positions of the different PCR amplification units A1 (−449 to −289), A2 (−247 to +63 of GFP), and A3 (GFP) are indicated by horizontal bars. Formaldehyde-cross-linked chromatin obtained from WT (+/+) BMMC, W^{sh}/W^{sh} BMMC, 32D cells, lin$^-$ Kit$^+$ BM cells, and BMMC derived from *BAC200-Kit-GFP* (T20)/W^{sh}/W^{sh}, *BAC30-Kit-GFP* (T51)/W^{sh}/W^{sh}, and *BAC200-Δ5′HS-Kit-GFP* (T78) mice was immunoprecipitated with antibodies against acetylated forms of histones H3 and H4, and the amount of the immunoprecipitated and input DNA was assayed by semiquantitative PCR. The ratios of signals of bound versus input chromatin were determined with a phosphorimager and are represented in the histogram. The error bars represent the standard deviations from three independent ChIP experiments.

WT BMMC and myeloid 32D cells. Significant association of Pol II was observed with the HS3 region (Fig. 7) in the 5′ HS cluster region of WT mast cells. Next we investigated the association of Pol II with the *Kit* promoter in WT and $W^{sh/sh}$ BMMC and 32D myeloid cells. Strong Pol II association was detected in WT BMMC but not in BMMC from $W^{sh/sh}$ mice and in the 32D myeloid cells (Fig. 7). Thus, Pol II recruitment to the HS3 and to the *Kit* promoter regions correlates with *Kit* expression in BMMC. In addition, we wanted to determine whether the 5′ HS cluster induces Pol II recruitment to the *Kit* promoter. To investigate this question, we analyzed Pol II association with the promoter sequences in BMMC obtained from $W^{sh/sh}$ mice carrying the *BAC200-Kit-GFP* and *BAC30-Kit-GFP* transgenes and in *BAC200Δ5′HS-Kit-GFP* transgenic mice. ChIP analysis revealed a significant recruitment of Pol II to the promoter sequences in BMMC carrying the *BAC200-Kit-GFP* transgene but not in cells carrying the *BAC30-Kit-GFP* and the *BAC200-Δ5′HS-Kit-GFP* transgenes (Fig. 7). Therefore, these results indicate that in mast cells, association of Pol II with the HS3 region in the 5′ HS cluster correlates with RNA polymerase II recruitment to the promoter and transcriptional activation.

DISCUSSION

The *Kit* gene is expressed in hemato- and lymphopoietic progenitor cell populations, mast cells, and eosinophils and in gametogenesis and melanogenesis and in the pacemaker cells of the intestinal tract. In order to investigate the mechanisms controlling tissue-specific *Kit* gene expression, we previously characterized two different *Kit* expression mutations: W^{sh} and W^{57} (4, 14, 15). Molecular characterization of these mutations identified a far upstream 3′ breakpoint for the W^{sh} inversion at kb −72 and for W^{57} deletion endpoints at kb −34 to −38 and kb −146 to −147 upstream of the kit transcription start site. Since these mutations diminish or abolish Kit expression in

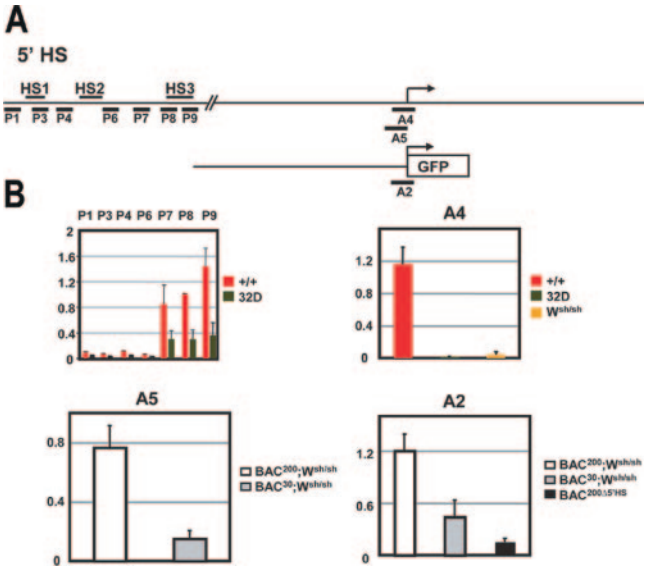

FIG. 7. Recruitment of RNA polymerase II to the chromatin of the 5′ HS cluster and in the *Kit* promoter region. A schematic representation of the *Kit* locus and the transgene constructs is shown at the top. The positions of the different PCR amplification units A2 (−247 to +63 of GFP), A4 (−247 to +37), and A5 (−247 to +3) and P1, P3, P4, P6, P7, P8, and P9 used for quantitation are indicated by horizontal bars. Formaldehyde-cross-linked chromatin obtained from WT (+/+) BMMC, W^{sh}/W^{sh} BMMC, 32D cells, and BMMC derived from *BAC200-Kit-GFP* (T20)/W^{sh}/W^{sh}, *BAC30-Kit-GFP* (T51)/W^{sh}/W^{sh}, and *BAC200-*Δ*5′HS-Kit-GFP* (T78) mice was immunoprecipitated with antibodies against RNA polymerase II, and the amount of immunoprecipitated and input DNA was assayed by semiquantitative PCR. The ratios of signals of bound versus input chromatin were determined with a phosphorimager and are represented in the histogram. The error bars represent the standard deviations from three independent ChIP experiments.

hematopoietic BM progenitors and BMMC, they were hypothesized to affect distant upstream control sequences of the *Kit* gene. To identify these remote *cis*-acting elements, we have generated *BAC-Kit-GFP* transgenic reporter mice carrying 200 kb of *Kit* upstream and 60-kb *Kit* coding sequences. Analysis of *Kit-GFP* reporter expression in these mice revealed expression in the brain, testis, oocytes, skin, peritoneal and bone marrow mast cells, and melanocytes at levels and in a pattern comparable to those of the endogenous *Kit* gene. These results suggested that, in these tissues, the *BAC200-Kit-GFP* clone could establish its own stable chromatin environment irrespective of the transgene insertion site and was able to direct tissue-specific *Kit-GFP* expression.

In the bone marrow, the *Kit* gene is expressed in hematopoietic stem cells and hematopoietic lineage progenitors, but in more differentiated hematopoietic and lymphoid cell types, *Kit* expression is abolished, except in mast cells and eosinophils. However, in the *BAC200-Kit-GFP* transgenic mice described here, no full *Kit-GFP* reporter expression was evident in the lineage-negative fetal liver and BM progenitor compartment. In a recent study, Cairns et al. (12) utilized transgenic mice carrying a *Kit-GFP* reporter construct consisting of 6.7 kb 5′ upstream and 4.5-kb *Kit* downstream sequences to investigate regulatory mechanisms of *Kit* gene expression in vivo. In these mice, hematopoietic progenitors in the fetal liver and in the BM were found to express the GFP reporter, suggesting that this fragment is sufficient to drive expression in early hematopoietic cells. Lineage commitment in hematopoiesis is regulated mainly at the transcriptional level involving positive and negative regulatory mechanisms (24, 38, 44, 46). It is possible that the *BAC200-Kit-GFP* transgene includes upstream and/or downstream negative regulatory elements that abrogate *Kit* gene expression in the hematopoietic progenitors. Furthermore, sequences not present in the *BAC200-Kit-GFP* transgene may be required for faithful *Kit* gene expression in hematopoietic BM progenitors. Significantly, the sorted Kit^+ GFP^- BM cells gave rise to GFP^+ BMMC, indicating that this population contains the mast cell progenitors. Thus, positive and negative regulatory sequences are critical in the regulation of *Kit* gene expression, likely involving different transcription factors and silencing mechanisms.

Deletion analysis of the upstream sequences in the *BAC200-Kit-GFP* transgene indicated that 3 kb of 5′ upstream sequences was insufficient to establish consistent GFP reporter expression in the transgenic mice. In contrast, inclusion of 30-kb upstream sequences gave reproducible and copy number-dependent expression of the GFP reporter in brain, testis, and oocytes, although there was no expression of the reporter in BMMC. Therefore, the lack of GFP expression in mast cells in these mice appears to recapitulate the Kit-negative mast cell phenotype in the W^{sh} and W^{57} mutant mice. It has been argued previously that the W^{sh} and W^{57} mutations result from position effects, but our observations here imply that the phenotypes of these mutations result from deletion of *cis*-acting control elements contained within the upstream *BAC200-Kit-GFP* sequences and not from position effects (3).

DNase I-hypersensitive regions in chromatin are often associated with gene regulatory sequences, such as enhancers, promoters, and locus control regions (16, 17). On the basis of our previous identification of a DNase I-hypersensitive site cluster in mast cells and melanocytes 147 to 154 kb upstream of the *Kit* transcription start site, we investigated the roles of these sequences in mediating *Kit* gene expression in vivo by generating BAC transgenic mice lacking these sequences. The lack of GFP reporter expression in BMMC implies that the 5′ HS cluster region includes *cis* regulatory sequences critical for *Kit* expression in mast cells. Furthermore, the copy number-dependent and position-independent expression of the GFP reporter gene in the *BAC200-Kit-GFP* transgenic mice suggests that these sequences constitute a locus control region, essential for *Kit* expression in mast cells.

A critical step in transcriptional activation of a gene is the remodeling of the chromatin from a condensed structure into an open structure. For a long time, DNase I hypersensitivity had been used to identify open chromatin structures. More recent work has identified modifications of the core histones H3 and H4 as indicators of chromatin remodeling. These modifications include histone H3 and H4 hyperacetylation and H3 K4 methylation. Our analysis of histone H3 and H4 hyperacetylation patterns in the 5′ HS cluster region and the proximal promoter of transcriptionally active WT BMMC showed a broad hyperacetylation pattern in the 5′ HS cluster region and strong hyperacetylation in the proximal promoter, whereas no hyperacetylation in the 5′ HS cluster region and in the proximal promoter of the inactive myeloid 32D cells was observed. Importantly, in Kit^+ lin^- BM cells, the proximal promoter was

hyperacetylated in agreement with *Kit* promoter activity in these cells, but the 5′ HS cluster region was not hyperacetylated. In this regard, it is of interest to note that the 5′ HS cluster in BMMC from $W^{sh/sh}$ mutant mice, in which more than 2 cM (far distal) of the *Kit* transcription start site was removed as a result of the chromosomal inversion, is hyperacetylated, even though *Kit* expression in these cells is abolished. Therefore, chromatin acetylation of the 5′ HS cluster region may be independent of its position relative to the *Kit* transcription start site and represent an epigenetic modification preventing chromatin from adopting a closed conformation. However, these results may also imply that chromatin remodeling in the 5′ HS cluster in mast cells precedes transcriptional activation of the *Kit* gene.

Analysis of acetylation of histones H3 and H4 in BMMC isolated from $W^{sh/sh}$ and *BAC200-Kit-GFP* transgenic mice indicated strong hyperacetylation in the *Kit* promoter of the reporter constructs, which is in agreement with the strong hyperacetylation pattern of the *Kit* promoter observed in the WT BMMC. In contrast, no hyperacetylation was observed in $W^{sh/sh}$, *BAC200-Kit-GFP*, and *BAC200-Δ5′HS-Kit-GFP* BMMC that lack GFP reporter gene expression. These results clearly indicate that the 5′ HS sequences are critical for driving mast cell *Kit* expression and mediating the chromatin remodeling in the *Kit* promoter region.

The impact of LCR deletions on promoter acetylation has been investigated in different systems. Deletion of the murine β-globin gene LCR does not affect hyperacetylation of the globin promoter, implying that acetylation of the β-globin gene promoter is independent of LCR function (42, 43). In contrast, at the human growth locus, hGH, deletion of HS1 in the LCR resulted in a loss of acetylation of the hGH-N promoter (23). Thus, similar to the hGH gene, hyperacetylation of the *Kit* promoter may reflect transcription and indicate that promoter activation follows LCR hyperacetylation. Furthermore, our results suggest that interaction between the 5′ HS sequences and the *Kit* promoter are necessary for acetylation in the promoter region, facilitating the recruitment of the basal transcriptional machinery and the binding of transcriptional activators.

LCRs may recruit transcription factors and components of the transcription preinitiation complex, including RNA polymerase II, that are subsequently transferred to the promoter region (25, 32, 47). Our finding that Pol II is bound to HS3 in the 5′ HS cluster and the promoter region in WT mast cells and BMMC isolated from $W^{sh/sh}$ and *BAC200-Kit-GFP* transgenic mice, but not in the promoter of the GFP-negative BMMC isolated from $W^{sh/sh}$, *BAC30-Kit-GFP*, and *BAC200-Δ5′HS-Kit-GFP* mice, is consistent with such a mechanism. In the β-globin locus, deletion of the LCR results in a loss of expression, but hyperacetylation and assembly of the transcription preinitiation complex at the promoter are not affected (42). In contrast, in the *Kit* gene, the 5′ HS cluster sequences are essential for both hyperacetylation of the *Kit* promoter and Pol II recruitment.

Chromatin remodeling is likely a prerequisite for recruitment of Pol II; therefore, we compared the patterns of H3 and H4 acetylation with the pattern of Pol II recruitment in the 5′ HS cluster region (Fig. 7B). Interestingly, the sites of Pol II association did not necessarily correlate with sites enriched for H3 and H4 acetylation, and this is in agreement with findings in the β-globin locus (26). Pol II binding was detected exclusively in the HS3 region, whereas histone acetylation was more broadly distributed throughout the 5′ HS cluster region (Fig. 5 and 7). On the basis of these findings, it had been proposed that Pol II recruitment at hypersensitive sites in the LCR is mediated by *trans*-acting factors, rather than by interaction with acetylated lysine residues of H3 and H4.

In summary, our studies of the mechanism of *Kit* receptor expression have identified a mast cell-specific LCR located 147 to 154 kb upstream of the *Kit* transcription start site. The demonstration of mast cell-specific chromatin remodeling and histone hyperacetylation in the LCR implies a transcriptionally competent chromatin state. Consequently, these modifications could make the LCR accessible to the transcription factors and components of the transcription preinitiation complex, including RNA polymerase II. Furthermore, activation of the *Kit* promoter might be a consequence of direct or indirect interaction between the LCR and the promoter region. Many different models have been described to explain distant effects, including looping, linking, and tracking. In any case, enhancer-promoter communication appears to be required for the assembly of promoter initiation complexes, which then initiate *Kit* transcription in mast cells. The identification and characterization of factors that mediate cell type-specific transcriptional activation of the *Kit* gene are of great interest and will be a challenge of the future.

ACKNOWLEDGMENTS

We thank Elizabeth Lacy and Willie Mark and their staff for their help in generating BAC transgenic mice, Antoinette Rookard for her help maintaining the mouse colony, Yasemine Yozgat and Prathima Nandivada for technical assistance. We thank Jan Hendrix for help with FACS analysis and Sandra Gonzales and Zsolt Lasar of the Molecular Cytology Facility for help with histological analysis. Furthermore, we thank Nat Heintz for advice and reagents for the generation of BAC constructs. We thank members of the laboratory of Elaine Fuchs for helpful discussions and Daniel Besser, Ines Ibanez-Talon, Imke Ehlers, and Eva Besmer for many useful discussions and comments on the manuscript.

This work was supported by grants from the National Institutes of Health, HL/DK55748 and DH38908 (to P.B.). C.B. is a NATO Postdoctoral Fellow.

REFERENCES

1. **Agosti, V., S. Corbacioglu, I. Ehlers, C. Waskow, G. Sommer, G. Berrozpe, H. Kissel, C. M. Tucker, K. Manova, M. A. Moore, H. R. Rodewald, and P. Besmer.** 2004. Critical role for Kit-mediated Src kinase but not PI 3-kinase signaling in pro T and pro B cell development. J. Exp. Med. **199:**867–878.
2. **Bachvarova, R. F., K. Manova, and P. Besmer.** 1993. Role in gametogenesis of c-kit encoded at the W locus of mice. Wiley-Liss, New York, N.Y.
3. **Bedell, M. A., N. A. Jenkins, and N. G. Copeland.** 1996. Good genes in bad neighbourhoods. Nat. Genet. **12:**229–232.
4. **Berrozpe, G., I. Timokhina, S. Yukl, Y. Tajima, M. Ono, A. D. Zelenetz, and P. Besmer.** 1999. The W(sh), W(57), and Ph Kit expression mutations define tissue-specific control elements located between −23 and −154 kb upstream of Kit. Blood **94:**2658–2666.
5. **Besmer, P.** 1997. Kit-ligand-stem cell factor. Marcel Dekker, New York, N.Y.
6. **Besmer, P.** 1991. The kit ligand encoded at the murine Steel locus: a pleiotropic growth and differentiation factor. Curr. Opin. Cell Biol. **3:**939–946.
7. **Besmer, P., K. Manova, R. Duttlinger, E. J. Huang, A. Packer, C. Gyssler, and R. F. Bachvarova.** 1993. The kit-ligand (steel factor) and its receptor c-kit/W: pleiotropic roles in gametogenesis and melanogenesis. Dev. Suppl. **1993:**125–137.
8. **Blanpain, C., W. E. Lowry, A. Geoghegan, L. Polak, and E. Fuchs.** 2004. Self-renewal, multipotency, and the existence of two cell populations within an epithelial stem cell niche. Cell **118:**635–648.
9. **Broudy, V. C.** 1997. Stem cell factor and hematopoiesis. Blood **90:**1345–1364.
10. **Buehr, M., A. McLaren, A. Bartley, and S. Darling.** 1993. Proliferation and

migration of primordial germ cells in We/We mouse embryos. Dev. Dyn. **198:**182–189.
11. **Bulger, M., and M. Groudine.** 1999. Looping versus linking: toward a model for long-distance gene activation. Genes Dev. **13:**2465–2477.
12. **Cairns, L. A., E. Moroni, E. Levantini, A. Giorgetti, F. G. Klinger, S. Ronzoni, L. Tatangelo, C. Tiveron, M. De Felici, S. Dolci, M. C. Magli, B. Giglioni, and S. Ottolenghi.** 2003. Kit regulatory elements required for expression in developing hematopoietic and germ cell lineages. Blood **102:**3954–3962.
13. **Chabot, B., D. A. Stephenson, V. M. Chapman, P. Besmer, and A. Bernstein.** 1988. The proto-oncogene c-kit encoding a transmembrane tyrosine kinase receptor maps to the mouse W locus. Nature **335:**88–89.
14. **Duttlinger, R., K. Manova, G. Berrozpe, T. Y. Chu, V. DeLeon, I. Timokhina, R. S. Chaganti, A. D. Zelenetz, R. F. Bachvarova, and P. Besmer.** 1995. The Wsh and Ph mutations affect the c-kit expression profile: c-kit misexpression in embryogenesis impairs melanogenesis in Wsh and Ph mutant mice. Proc. Natl. Acad. Sci. USA **92:**3754–3758.
15. **Duttlinger, R., K. Manova, T. Y. Chu, C. Gyssler, A. D. Zelenetz, R. F. Bachvarova, and P. Besmer.** 1993. W-sash affects positive and negative elements controlling c-kit expression: ectopic c-kit expression at sites of kit-ligand expression affects melanogenesis. Development **118:**705–717.
16. **Felsenfeld, G., J. Boyes, J. Chung, D. Clark, and V. Studitsky.** 1996. Chromatin structure and gene expression. Proc. Natl. Acad. Sci. USA **93:**9384–9388.
17. **Fraser, P., and F. Grosveld.** 1998. Locus control regions, chromatin activation and transcription. Curr. Opin. Cell Biol. **10:**361–365.
18. **Galli, S. J., K. M. Zsebo, and E. N. Geissler.** 1994. The kit ligand, stem cell factor. Adv. Immunol. **55:**1–96.
19. **Geissler, E. N., M. A. Ryan, and D. E. Housman.** 1988. The dominant-white spotting (W) locus of the mouse encodes the c-kit proto-oncogene. Cell **55:**185–192.
20. **Gokkel, E., Z. Grossman, B. Ramot, Y. Yarden, G. Rechavi, and D. Givol.** 1992. Structural organization of the murine c-kit proto-oncogene. Oncogene **7:**1423–1429.
21. **Grosveld, F., G. B. van Assendelft, D. R. Greaves, and G. Kollias.** 1987. Position-independent, high-level expression of the human beta-globin gene in transgenic mice. Cell **51:**975–985.
22. **Grunstein, M.** 1997. Histone acetylation in chromatin structure and transcription. Nature **389:**349–352.
23. **Ho, Y., F. Elefant, N. Cooke, and S. Liebhaber.** 2002. A defined locus control region determinant links chromatin domain acetylation with long-range gene activation. Mol. Cell **9:**291–302.
24. **Hu, M., D. Krause, M. Greaves, S. Sharkis, M. Dexter, C. Heyworth, and T. Enver.** 1997. Multilineage gene expression precedes commitment in the hemopoietic system. Genes Dev. **11:**774–785.
25. **Johnson, K. D., H. M. Christensen, B. Zhao, and E. H. Bresnick.** 2001. Distinct mechanisms control RNA polymerase II recruitment to a tissue-specific locus control region and a downstream promoter. Mol. Cell **8:**465–471.
26. **Johnson, K. D., J. A. Grass, C. Park, H. Im, K. Choi, and E. H. Bresnick.** 2003. Highly restricted localization of RNA polymerase II within a locus control region of a tissue-specific chromatin domain. Mol. Cell. Biol. **23:**6484–6493.
27. **Kent, W. J., C. W. Sugnet, T. S. Furey, K. M. Roskin, T. H. Pringle, A. M. Zahler, and D. Haussler.** 2002. The human genome browser at UCSC. Genome Res. **12:**996–1006.
28. **Kluppel, M., J. D. Huizinga, J. Malysz, and A. Bernstein.** 1998. Developmental origin and Kit-dependent development of the interstitial cells of Cajal in the mammalian small intestine. Dev. Dyn. **211:**60–71.
29. **Kluppel, M., D. L. Nagle, M. Bucan, and A. Bernstein.** 1997. Long-range genomic rearrangements upstream of Kit dysregulate the developmental pattern of Kit expression in W57 and Wbanded mice and interfere with distinct steps in melanocyte development. Development **124:**65–77.
30. **Kondo, M., A. J. Wagers, M. G. Manz, S. S. Prohaska, D. C. Scherer, G. F. Beilhack, J. A. Shizuru, and I. L. Weissman.** 2003. Biology of hematopoietic stem cells and progenitors: implications for clinical application. Annu. Rev. Immunol. **21:**759–806.
31. **Kuo, M. H., J. Zhou, P. Jambeck, M. E. Churchill, and C. D. Allis.** 1998. Histone acetyltransferase activity of yeast Gcn5p is required for the activation of target genes in vivo. Genes Dev. **12:**627–639.
32. **Leach, K. M., K. Nightingale, K. Igarashi, P. P. Levings, J. D. Engel, P. B. Becker, and J. Bungert.** 2001. Reconstitution of human beta-globin locus control region-hypersensitive sites in the absence of chromatin assembly. Mol. Cell. Biol. **21:**2629–2640.
33. **Li, Q., K. R. Peterson, X. Fang, and G. Stamatoyannopoulos.** 2002. Locus control regions. Blood **100:**3077–3086.
34. **Maeda, H., A. Yamagata, S. Nishikawa, K. Yoshinaga, S. Kobayashi, and K. Nishi.** 1992. Requirement of c-kit for development of intestinal pacemaker system. Development **116:**369–375.
35. **Manova, K., and R. F. Bachvarova.** 1991. Expression of c-kit encoded at the W locus of mice in developing embryonic germ cells and presumptive melanoblasts. Dev. Biol. **146:**312–324.
36. **Mellor, J.** 2005. The dynamics of chromatin remodeling at promoters. Mol. Cell **19:**147–157.
37. **Misulovin, Z., X. W. Yang, W. Yu, N. Heintz, and E. Meffre.** 2001. A rapid method for targeted modification and screening of recombinant bacterial artificial chromosome. J. Immunol. Methods **257:**99–105.
38. **Miyamoto, T., H. Iwasaki, B. Reizis, M. Ye, T. Graf, I. L. Weissman, and K. Akashi.** 2002. Myeloid or lymphoid promiscuity as a critical step in hematopoietic lineage commitment. Dev. Cell **3:**137–147.
39. **Nagle, D. L., C. A. Kozak, H. Mano, V. M. Chapman, and M. Bucan.** 1995. Physical mapping of the Tec and Gabrb1 loci reveals that the Wsh mutation on mouse chromosome 5 is associated with an inversion. Hum. Mol. Genet. **4:**2073–2079.
40. **Nagle, D. L., P. Martin-DeLeon, R. B. Hough, and M. Bucan.** 1994. Structural analysis of chromosomal rearrangements associated with the developmental mutations Ph, W19H, and Rw on mouse chromosome 5. Proc. Natl. Acad. Sci. USA **91:**7237–7241.
41. **Sanders, K. M., T. Ordog, S. D. Koh, S. Torihashi, and S. M. Ward.** 1999. Development and plasticity of interstitial cells of Cajal. Neurogastroenterol. Motil. **11:**311–338.
42. **Sawado, T., J. Halow, M. A. Bender, and M. Groudine.** 2003. The beta-globin locus control region (LCR) functions primarily by enhancing the transition from transcription initiation to elongation. Genes Dev. **17:**1009–1018.
43. **Schubeler, D., C. Francastel, D. M. Cimbora, A. Reik, D. I. Martin, and M. Groudine.** 2000. Nuclear localization and histone acetylation: a pathway for chromatin opening and transcriptional activation of the human beta-globin locus. Genes Dev. **14:**940–950.
44. **Smale, S. T.** 2003. The establishment and maintenance of lymphocyte identity through gene silencing. Nat. Immunol. **4:**607–615.
45. **Strahl, B. D., and C. D. Allis.** 2000. The language of covalent histone modifications. Nature **403:**41–45.
46. **Tagoh, H., A. Schebesta, P. Lefevre, N. Wilson, D. Hume, M. Busslinger, and C. Bonifer.** 2004. Epigenetic silencing of the c-fms locus during B-lymphopoiesis occurs in discrete steps and is reversible. EMBO J. **23:**4275–4285.
47. **Vieira, K. F., P. P. Levings, M. A. Hill, V. J. Crusselle, S. H. Kang, J. D. Engel, and J. Bungert.** 2004. Recruitment of transcription complexes to the beta-globin gene locus in vivo and in vitro. J. Biol. Chem. **279:**50350–50357.
48. **Waskow, C., S. Paul, C. Haller, M. Gassmann, and H. Rodewald.** 2002. Viable c-Kit(W/W) mutants reveal pivotal role for c-Kit in the maintenance of lymphopoiesis. Immunity **17:**277–288.
49. **Weintraub, H., and M. Groudine.** 1976. Chromosomal subunits in active genes have an altered conformation. Science **193:**848–856.
50. **Yang, D., C. Tournier, M. Wysk, H. T. Lu, J. Xu, R. J. Davis, and R. A. Flavell.** 1997. Targeted disruption of the MKK4 gene causes embryonic death, inhibition of c-Jun NH_2-terminal kinase activation, and defects in AP-1 transcriptional activity. Proc. Natl. Acad. Sci. USA **94:**3004–3009.
51. **Yang, X. W., P. Model, and N. Heintz.** 1997. Homologous recombination based modification in *Escherichia coli* and germline transmission in transgenic mice of a bacterial artificial chromosome. Nat. Biotechnol. **15:**859–865.